



# The Impacts of Population Dynamics on Land Use using GIS and RS (Case Study of Amman, Jordan)

**Ahmad Hussein N. Al Naimat**

Research Scholar, DOS in Geography, University of Mysore.

**Prof. Dr. H. Nagaraj**

Research Guide and Professor of in Geography, DOS in Geography, University of Mysore.

## Abstract

One of the most important factors in the changes in land use is the population dynamic effects. Through the treatment of spatial visuals for the years 1975 and 1984 to 2019 and data from the global signature system and topographic maps, the results indicated an increase in the population by % from 1975 to 1984 in addition to an increase in the proportion of land cultivated %

Keywords: GIS, Land Use, Landsat, Population of Jordan, Jordan

## 1. Introduction

The urban population varies spatially and temporally, in size and composition, within cities and between cities. In developing countries in the Middle East, especially in Jordan, the urban population is usually dense around city centers and dispersed in the suburbs, and is growing rapidly on the urban margins.

Due to the complex relationships between urban dwellers and the entire human environmental system, differences in urban population, their causes and impacts, are difficult to explain, predict, or influence.

Neighborhood differences are so important in urban studies as findings and impacts on economic, social and environmental conditions in cities and in the areas to which cities are connected this is why.

## 2. Methods

### 2.1 Study Area

It is a common concept of land use and its uses. So does the relationship between man and the earth represent this relationship affected by temporal and spatial factors and variables, and the capital Amman is considered one of the areas that witnessed a significant urban change and expansion, and the variety of land uses varied between quarries of stone (quarries), residential areas, forests, trees, lands Rugged, unused lands.

Amman city is chosen as the study area is the capital city of Jordan. It covers a total area of 758.85 km<sup>2</sup> and consists of 22 districts. It is one of the most densely populated places in the Jordan, the estimated population of Amman was approximately 4.090 million inhabitants (in 2017), is located between latitude (31°45'00" - 32°05'00") North and longitude (35°44'00" - 36°14'00") East Amman is located on an undulating plateau that comprises the northwest of Jordan.

The topography of the city consists of a series of steep hills and deep and sometimes narrow valleys. Limestone rocks intermeddled with chart, marl, and chalk beds are the dominant rocks in the study area. The soil in the studied area is derived from limestone, and the soil depth decreases as the inclination becomes steeper than 4%. The most important characteristics of this soil are high proportions of silt and calcium carbonates (Dinka, Chaka, 2019). Vegetation in the study area includes irrigated vegetables and rain-fed crops of wheat, barley, olives, and fruit trees. Deciduous and evergreen oaks and pine forests are scattered in the western parts of the study area. The eastern parts are used as open rangelands (Hussain, Mubeen, Ahmad, et al., 2019).

### 2.2 Data Collection

While studying past population growth, many questions come to mind. For example, how have population trends tend to vary within Jordan's major urban areas since 1954? How can we compare spatial extent and patterns of different trends in different urban areas? What is the rate of spatial and temporal analysis of population change from the macro (regional) level to the micro level? Previous research on population distribution, particularly the structure and dynamics of urban population density, provides some answers to these questions, both theoretically and empirically, but no previous work has directly addressed these questions on a large spatial and temporal scale.

The relationship between population and development is an interactive relationship whereby the country's population, growth rates, demographic and economic characteristics, and their geographical distribution affect the development potential in general and the opportunities to improve the quality of life and reduce poverty, which makes it difficult for many countries to exit the vicious cycle where population increase leads to Poor development and an increase in poverty rates on the one hand, and on the other hand, the environment in which development is absent and in which poverty increases, population growth rates rise.

The city of Amman, “the capital of the Hashemite Kingdom of Jordan” in general, and the study area “Liwa al-Jamaa” in particular, has witnessed significant population changes during the last quarter of the twentieth century and the beginning of the current century, as the population of Amman increased from 600,284 in 1979 to about 2,473,400 in the year While the population of the university district increased from 39,383 people in 1979 to about 355,790 people in 2012, the Department of Statistics, 2012 estimates. (The region also witnessed an increase in the natural population growth rate and the rate of migration to it, whether it was internal migration

The return of hundreds of thousands of Jordanian expatriates after the Gulf War in 1991, which led to rapid population growth and random population distribution, which in turn led to the emergence of informal areas and neighborhoods, and this requires the development of appropriate plans to face these sudden population changes and the resulting problems And that is by encouraging official institutions to conduct periodic and detailed surveys, which allows researchers to study population changes in detail for those cities or regions.

The population estimates between the 2004 & 2015 Population & Housing Censuses were based on the results of the General Population & Housing Census 2015. The population growth rate showed a significant increase to 5.3% during the period 2004 – 2015)

### **2.3 Obtaining Landsat Data**

The USGS Global Visualize Viewer program operated by Earth Resources Observation and Science (EROS) is the primary browser for downloading / requesting Landsat data. It now provides all Landsat 1-5 and 7 users with archiving data for free, using a data product standard recipe. Earth Explorer<sup>8</sup> and GIOVIS<sup>9</sup> are extremely effective for browsing satellite imagery, providing access to satellite, aerial photography and mapping data products. It is important to note here that when selecting a suitable image, it can be downloaded once or applied to the USGS, as the scene in question is processed by the National Land Archives Production System (NLAPS). It takes a few days for a request to be responded to. In fact, during the application processing time systematic, radiological and engineering corrections are generated, using both ground control points and a digital elevation model (DEM), which is time consuming.

The aforementioned satellite images were chosen based on the following:

A- The type of sensor carried on the satellite according to its stages of development, from the sensor (Landsat 1-5 MMS) to the sensor (Landsat 8 OLI-TIRS).

B- The time of capturing the satellite images, so that the date of capture was close to the dry season of the year in Jordan, so that the results are uniform on the one hand. On the other hand, they are devoid of clouds. The clouds appear in the study area, starting from the month of October, and reaching their maximums in the months of December and April, and this is due to the increase in the number of depressions reaching the study area.

C- The need for research to make comparisons and reveal the changes that occurred for each (10) years and during (44 years) of (1975 to 2019).

D- The geometrically corrected images that are free from geometric and radiometric defects, as available on the official website of the NASA Agency (USGS).

It was possible to obtain all the satellite images for the years (1975 - 2019) through its website (<https://earthexplorer.usgs.gov/>) after registration and download for the views. For this research, twelve Landsat scenes were downloaded - Two MSS scenes for 1975 and four TM scenes for 1984 and 1994 (two per year) at various times during the first and second years of the current search. It should be noted here that the years of these pictures were chosen taking into account the dates of the Amman census. Table 2.5-1 presents the date and specifications of the used satellite data.

**Table 1: The Numbers and Dates of Satellite Images used in the Study Locations**

Scene ID	Satellite image Type	Acquisition Date
LM02_L1TP_187038_19750629_2018 0425_01_T2	Landsat 1-5 MMS C1 Level-1	6/29/1975
LM02_L1TP_186038_19750628_2018 0425_01_T2	Landsat 1-5 MMS C1 Level-1	6/28/1975
LT05_L1TP_173038_19840627_20171 213_01_T1	Landsat 4-5 TM C1 Level-1	6/27/1984
LT05_L1TP_174038_19840618_20171 213_01_T1	Landsat 4-5 TM C1 Level-1	6/18/1984
LT05_L1TP_173038_19940420_20180 208_01_T1	Landsat 4-5 TM C1 Level-1	4/20/1994
LT05_L1TP_174038_19940411_20180 208_01_T1	Landsat 4-5 TM C1 Level-1	4/11/1994

## 2.4 Data Resolution and Analysis:

Various parameters of data resolution such as spatial, spectral, radiometric and temporal resolutions are very important in change detection studies. They therefore need to be examined carefully. For instance, spatial resolution of the satellite data in land cover classification is an important consideration, as it dictates the size of the feature that can be detected in the image. Spatial resolution is also described as the instantaneous field of view (IFOV) of the sensor and it is a measure of the area viewed by a single detector. IFOV measures the “ground resolution cell” i.e. a view of the one section of the ground that emitted energy back to the sensors. Therefore, the IFOV of sensors is a good measure to make a comparison among different sensors (Jensen, 2005). Landsat imagery is considered to be of medium resolution, and many researchers recommend Landsat, particularly Landsat TM as most suitable for urban studies (Jat et al. 2008; Zhang et al 2006; Lo and Nobel, 1990). IFOV is mathematically calculated as:

$$\text{IFOV} = \frac{HD}{f} \dots\dots\dots (\text{Townshend et al., 1998})$$

Whereas D= Detector size, H= Flying height above the earth and f= Focal length of a scanner

Spectral resolution of an image refers to the specific wavelength intervals in the electromagnetic spectrum. Narrow intervals in the electromagnetic spectrum refer to the spectral resolution fine, and wider intervals are referred to as coarse spectral resolution. For instance, band 3 of Landsat TM records energy between 0.63 to 0.69  $\mu\text{m}$ , therefore due to narrow interval its spectral resolution is considered to be fine, as compared to Band 1 of SPOT panchromatic which records between 0.51 to 0.73  $\mu\text{m}$ , and is considered to be a coarse spectral resolution band. It is important to note that many change detection algorithms do not function properly when bands of one sensor system do not match those of another system.

The radiometric resolution of an image refers to the number of possible file values in each band or in other words it characterizes the total energy that each band captures in a particular sensor. For example, Landsat TM records data in 8 bits, which means that the data file value or Digital Number (DN) of each pixel ranges from 0 to 255. This is much improved radiometric resolution as compared to Landsat MSS missions which recorded the data in 6 bits, containing DN values from 0 to 69. Particularly for comparison purposes, it is necessary to know the radiometric resolution of the data acquired. Temporal resolution, commonly known as the repeat cycle, refers to the amount of time taken by a sensor to return to a previously imaged location. For example, Landsat 4-7 views the same area of the globe once every 16 days. On the other hand, SPOT revisits, the same area after every three days. Temporal resolution is an important factor to consider in change detection studies, as temporal differences between remotely sensed images are not only caused by the changes in the spectral characteristics of the Earth's surface features / organisms, can also result from atmospheric differences and changes in the Sun's position during the day and during the year (Weng, 2012). The satellite data were temporarily selected to provide a phenological picture of the land cover of the study area over the different stages of development as well as sufficient separation for changes to occur. Jensen and Cowen (1999) suggested that for such types of change detection studies multiple satellite images of different times during the same acoustic arrangement are ideal. Also, to reveal the type of urban development, it is preferable that the images be separated by at least five years (Coppin et al., 2004). The intent of this study was to select satellite data in an acoustic arrangement compatible with the organization of national censuses.

## 2.5 Conclusion:

Following statistical measures were applied to the Amman of the study area to compare the landscape patterns in the last three census periods to explain the land use /cover changes.

And In this study, both statistical and geospatial techniques were used. Thus the methodology adopted reflects the elements of satellite data, enumeration, qualitative data and GPS. In fact, the current study is a mixture of physical and human geography techniques. For example, on the one hand, it processes, analyzes, and evaluates satellite data using various algorithms and techniques for accuracy assessment, and on the other hand, it creates techniques for collecting and analyzing census data, qualitative and social data, using qualitative methods and statistical techniques. The difficult part of the methodology is to incorporate data that highlight changes in the study area. The methodology used in this

study can be summarized in five main steps. The first step focused on fieldwork methodology for collecting qualitative data, census and GPS. The second and important section of the methodology deals with the processing of satellite data. This section describes how remote sensing data has been corrected, geo-corrected, optimized and categorized using different classification techniques and algorithms. The third step focused on the classification scheme, classification procedures, and evaluation procedures for remote sensing data. Statistical measures of change detection techniques are described. He discussed the preparation and evaluation of transitional matrices to assess land cover change during different censuses. The mixed methods approach is adopted in the final section. This section was not limited to statistical analysis of population data, and land cover data extracted from images classified for remote sensing, but also addressed the integration of census data, remote sensing and geographic information systems in this step.

Accuracy assessment is an important factor in analyzing Landsat data and judging how successful a classifier is. To assess accuracy, reference data (land dirt) are required to define class types at specific locations and to identify and quantify mapping errors (Congalton & Green, 2008; Foody, 2010). Reference data sources in this study included ground research using GPS and GIS layers, qualitative data including interviews, focus group discussions, and topographic maps. Rating accuracy was performed by selecting a set of pixels on the rated image and comparing it to the actual image and ground reference data. The relationship between the two sets of information above was compared and summarized in the cell array. From the cell matrix, an error matrix and an accuracy report were derived. Two measures of error are derived from the error matrix, i.e., omission error or product accuracy and commission error or user accuracy. The resolution of the producer indicated the likelihood of a reference pixel being classified correctly. Estimated by dividing the total number of integer pixels in a class by the total number of pixels for that class. User resolution indicates the probability that the pixel rated on the image represents this class on Earth. Estimated by dividing the total number of correct pixels in a category by the total number of pixels that are classified in that category. In addition to the two measurements mentioned above, the overall accuracy is also found by dividing the total number of integer classes by the total number of classes. The kappa coefficient, which statistically measures the relationship between post-chance agreement and expected variance, and is an indication of the extent to which correct values of the error matrix are attributed to a "real" agreement versus a "chance" agreement, was also calculated using the following formula.

$$K = \frac{\text{Observed Correct} - \text{Expected Correct}}{1 - \text{Expected Correct}}$$

An assessment of the accuracy of the Landsat ETM image of Supervised classification for year 2004, which depended on the previously selected training models after making sure of their ability to separate the items, as mentioned previously, and by randomly sampling (100 samples) and making a comparison between the categorized visual and the reference image represented by the combined images. Panchromatic range for the same year with spatial resolution (15 meters) and obtain a Confusion matrix.

And based on the standard of total accuracy, it was found that it reached 86.60 % which is a very high percentage and Kappa Coefficient = 0.8326. Table (2-5).

**Table 2: Ground Truth using ENVI Software (Confusion Matrix, Prepared by the Researcher) (In Pixels)**

Class	Urban	Agricultural	Barren Land	Rangeland	Chert plain	Wadi	Exposed Rock
Urban	4298	136	0	178	0	0	2
Agricultural	26	5083	135	249	59	56	65
Rangeland	0	3796	5708	47	0	0	14
Barren Land	9	13	180	11947	154	43	347
Chert plain	6	2	0	0	28047	911	22
Wadi	0	19	20	25	2772	7293	1113
Exposed Rock	0	5	17	280	186	596	11874
Total	4339	9054	6060	12726	31218	8899	13437

**Table 3: Ground Truth using ENVI Software (Confusion Matrix, Prepared by the Researcher) (In Percent)**

Class	Urban	Agricultural	Barren Land	Rangeland	Chert plain	Wadi	Exposed Rock
Urban	99.06	1.5	0	1.4	0	0	0.01
Agricultural	0.6	56.14	2.23	1.96	0.19	0.63	0.48
Rangeland	0	41.93	94.19	0.37	0	0	0.1
Barren Land	0.21	0.14	2.97	93.88	0.49	0.48	2.58
Chert plain	0.14	0.02	0	0	89.84	10.24	0.16
Wadi	0	0.21	0.33	0.2	8.88	81.95	8.28
Exposed Rock	0	0.06	0.28	2.2	0.6	6.7	88.37
Total	100	100	100	100	100	100	100

**Table 4: Omission Percent of Confusion Matrix Done/Class Commission using ENVI Software**

Class	Commission (%)	Omission (%)	Commission (Pixel)	Omission (Pixel)
Urban	6.85	0.94	316/4614	41/4339
Agricultural	10.4	43.86	590/5673	3971/9054
Rangeland	40.32	5.81	3857/9565	352/6060
Barren Land	5.88	6.12	746/12693	779/12726
Chert plain	3.25	10.16	941/28988	3171/31218
Wadi	35.13	18.05	3949/11242	1606/8899
Exposed Rock	8.37	11.63	1084/12958	1563/13437

**Table 5: User Accuracy of Confusion Matrix/Class Producer Accuracy using ENVI Software**

Class	Prod. Acc. (%)	User Acc. (%)	Prod. Acc. (Pixel)	User Acc. (Pixel)
Urban	99.06	93.15	4298/4339	4298/4614
Agricultural	56.14	89.6	5083/9054	5083/5673
Rangeland	94.19	59.68	5708/6060	5708/9565
Barren Land	93.88	94.12	11947/12726	11947/12693
Chert plain	89.84	96.75	28047/31218	28047/28988
Wadi	81.95	64.87	7293/8899	7293/11242
Exposed Rock	88.37	91.63	11874/13437	11874/12958

By comparing the numerical classification with the visual classification, some things have been observed that represent deficiencies of some of their types as follows:

1. With regard to distinguishing linear and point phenomena: through the use of numerical classification, it did not distinguish them well, as is the case in transmission and communication lines, as is the case in distinguishing gas burning towers or refineries. As opposed to visual categorization, which can be distinguished well and precisely, especially when digital augmentation is used in the visual interpretation process.
2. The deficiency of the digital classification in isolating urban lands and buildings of regular geometric shapes from neighboring lands with similar reflectivity, which resulted in severe confusion over the classified images, for example, there has been an overlap between urban lands with bare lands and agricultural lands, because most of the urban roofs are formed from earthen materials.



3. The failure of the visual classification to distinguish the phenomena with weak contrasts, and the visual interpretation may be exposed to an optical illusion. In contrast to the numerical classification, which is better at distinguishing contrasts that are small and cannot be distinguished visually. This feature is represented by the unsupervised classification method, which gives more accurate results than the supervised classification. If the number of items is chosen well, it is able to distinguish areas that the mentor was not able to distinguish because they are not clear in the process of selecting training areas.

4. The deficiency of the unsupervised classification in isolating the sand dunes from sand sediments, although there is a difference in the reflectivity except after moving to the supervised classification.

5. There is a difference in areas in the supervised classification from unsupervised even if the same number of classes are chosen in both types, and also even if the training areas increased or decreased as well as seen in the following figures.

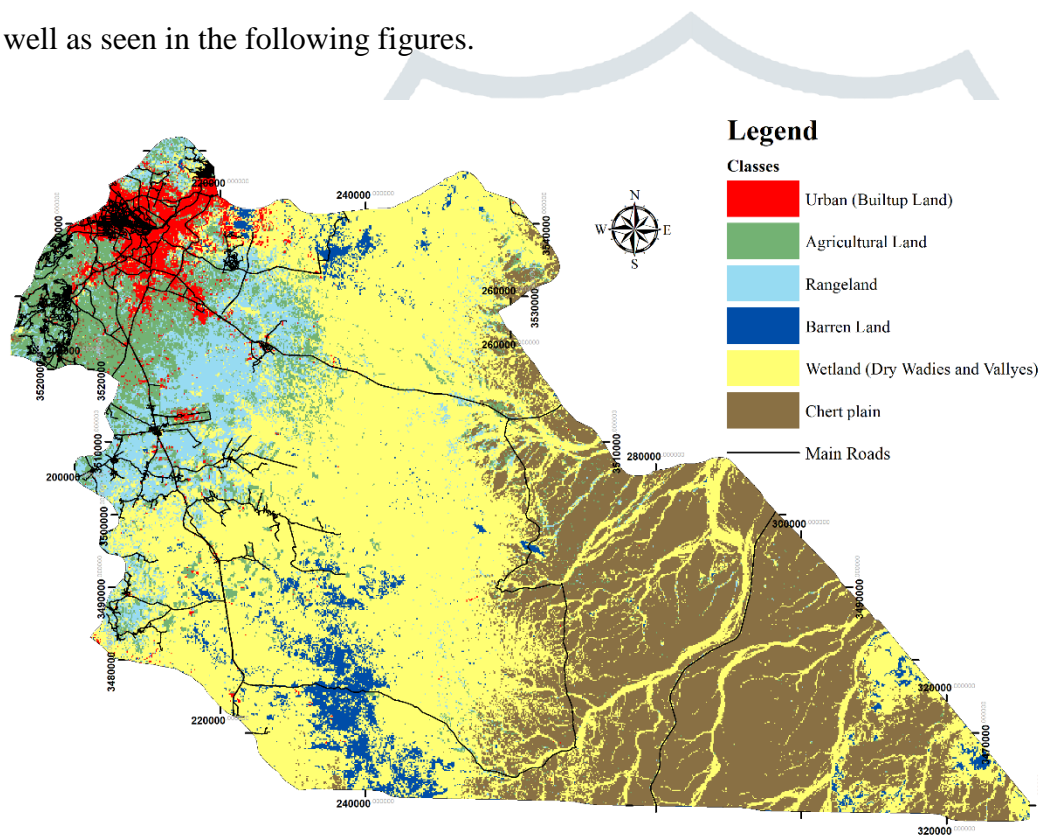


**Figure 1: +ETM for the Landsat (Maximum Likelihood) Image Supervised for Year 2004 IB5G4R – Classification Band Combination**

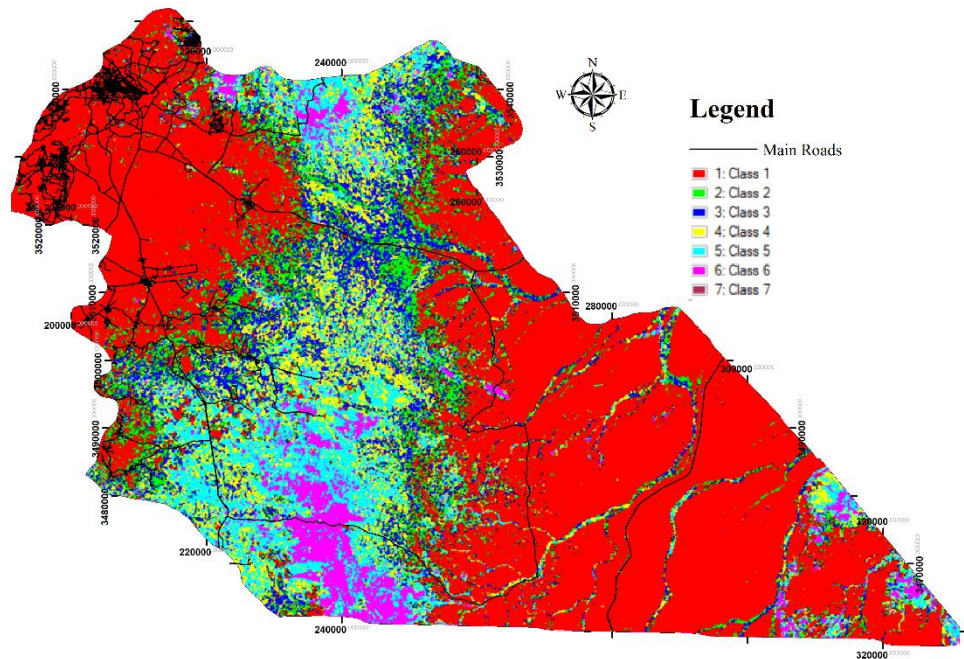


**Figure 2: R +ETM for the Landsat (ISODATA) Image Unsupervised Classification for Year 2004 IB5G4 Band Combination**

## 2.6 Change Detection Analysis Methods

The change in the land cover of the study area over a period of forty years is a response to social, economic and political forces. Information about the nature of the change in land use / coverage is essential to managing proper planning and resource regulations. Therefore, change detection is a major topic in the analysis of remote sensing images (Foody, 2002; Singh, 1989; Wong et al., 1997) and it is a major application of Landsat data. Change detection allows evaluating changes between images obtained at different times either visually or by using digital techniques. Digital technologies have the advantage of being easy to capture data into GIS.

Researchers use different algorithms to detect change depending on the type of applications, satellite sensors, areas, and targets of interest as well as the amount of detail required (Seto et al., 2002). The most popular change detection algorithms include:

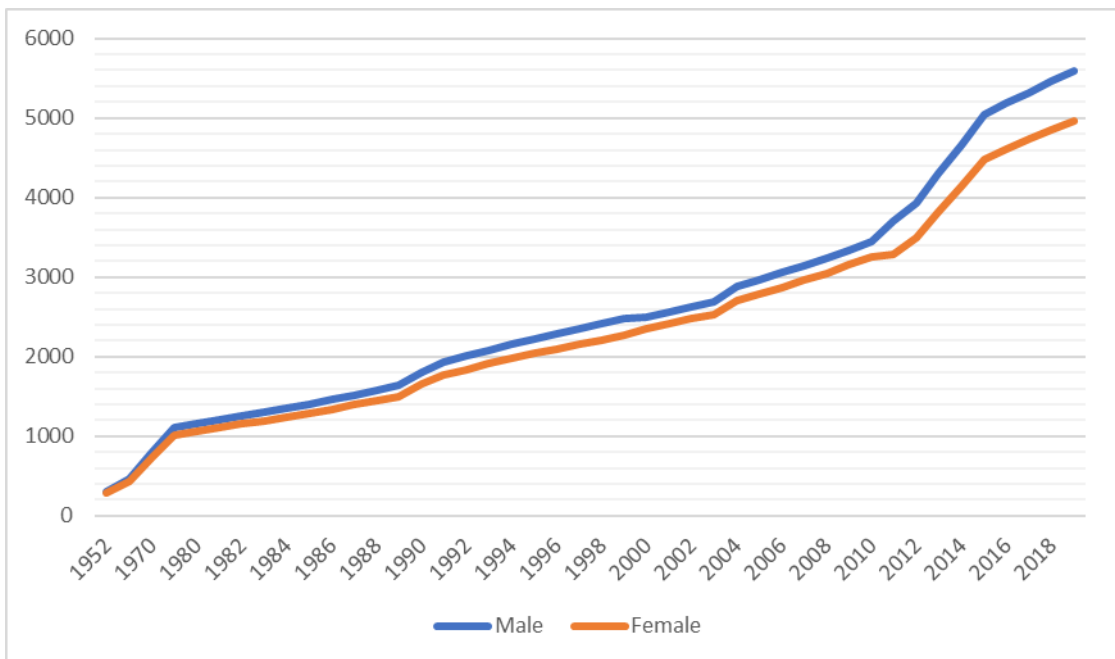
- Multi-date composite image comparisons
- Image Algebra (e.g. band differencing, band rationing, image regression)
- Post classification comparison
- Binary mask applied to date 2
- Cross correlation
- Visual on-screen digitization
- Knowledge based vision systems

- Chi-square transformation
- Write function memory insertion
- Spectral vector change analysis

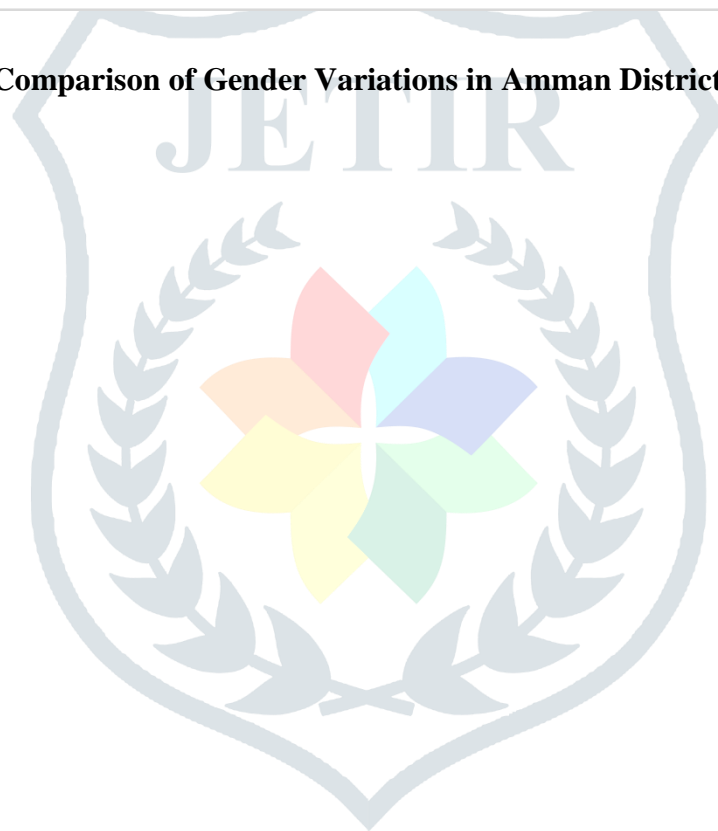
Each method has its own advantages and no single method can be considered perfect. For example, image marking is commonly used in forestry and agricultural studies (Fung & Chan 1994; Singh, 1989). Image kerning reduces the influence of topology such as shading and illumination and vector analysis reveals changes present in multi-spectral data inputs (Berberoglu and Akin, 2009). Incline methods reduce the harmful effects of variation in weather conditions (Coppin and Bauer 1996). High temporal contrast of the spectral characteristics of the main land cover types; The complexity of the scene due to the topographical differences of the study area and the difficulties of spectral separation of some ground covers due to their similar reflection, limits the use of some of the aforementioned change detection techniques in the study area. Therefore, to detect and measure changes in land cover and compare it with census data and government policies, a post-classification algorithm was applied to the study area. It has the following three advantages over the other methods.

- Does not require atmospheric correction
- Provides “from-to” change information
- Next base map is already created.

Shalaby and Tateshi (2007) apply post-classification change detection techniques to examine urban development in the northwest coastal areas of Egypt. And they used the Idrisi cross-classification function to perform the spatial distribution of the "from to" change information for different land cover. Using the above function, Munoz-Villers and Lopez-Blanco (2008) studied deforestation and agricultural land shifts in mountainous regions of Mexico. Shirazi (2012) used a post-classification method for a temporal analysis of land use and land cover changes in Lahore - Pakistan. Gosai (2009) publication classification found an appropriate method to detect change, while analyzing land use changes in Thimbo, Bhutan from 1990 to 2007.



**Figure 3: Comparison of Gender Variations in Amman District 1952-2019**



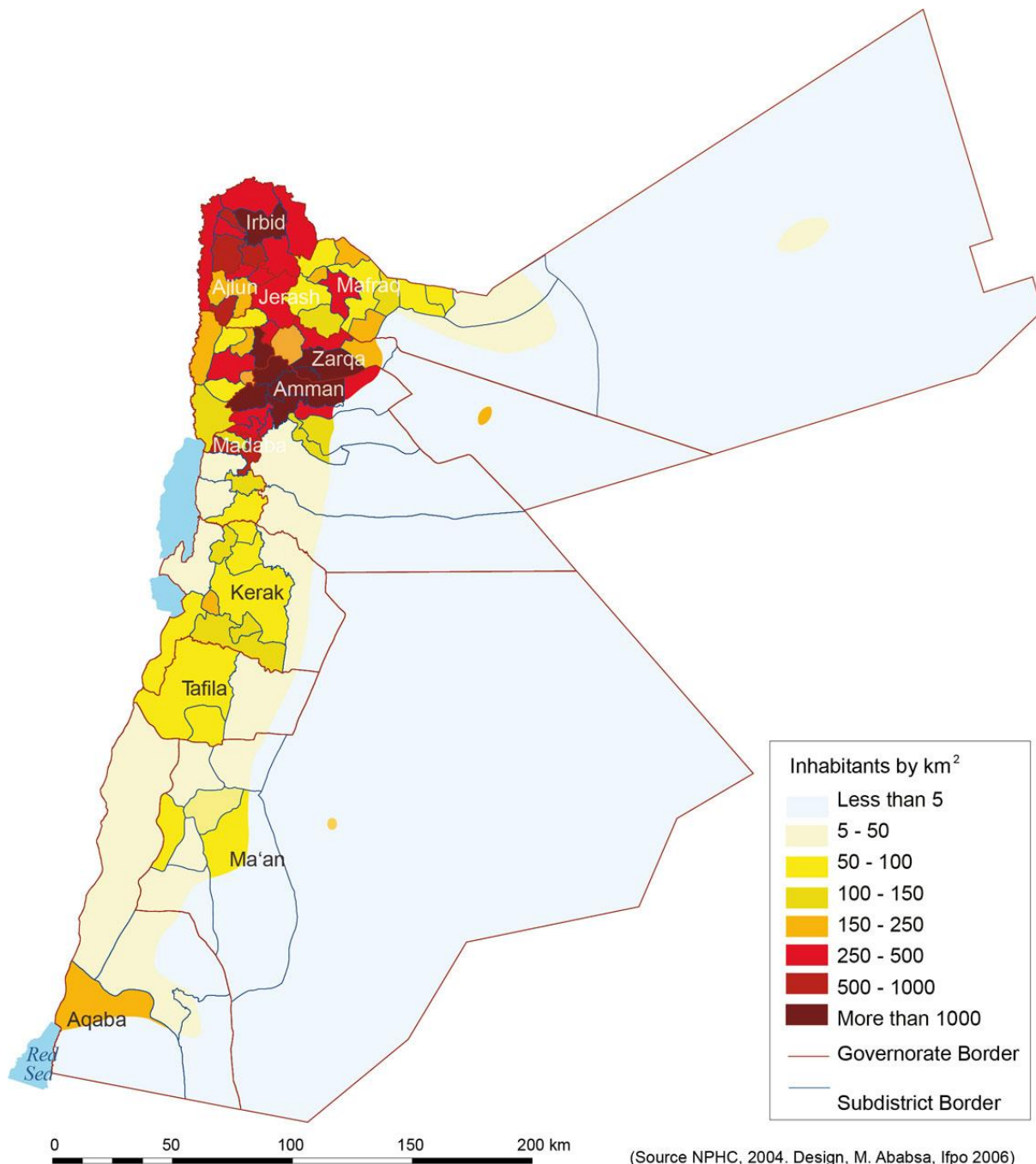


**Figure 5: Jordan Population Den by Governorate in 2010 (inhabitants per km<sup>2</sup>).**

The country's population density is 69 inhabitants per square kilometre. But 80% of the country has fewer than five inhabitants per square kilometre (roughly everywhere below the 100 mm isohyet). The entire population lives in an area of less than 10,000 km<sup>2</sup>, giving a true density ten times higher: over 650 inhabitants per square kilometre. The northern governorates, with less desert areas, have densities of over 300 inhabitants per km<sup>2</sup> and the figure reaches 962 in Irbid. Karak and Tafilah are in the mountains and have suffered from population drift towards the capital; they have respective population densities of 68 and 39 inhabitants per km<sup>2</sup>. In the cities, population density reaches world records with over 30,000 inhabitants per km<sup>2</sup> in the poor areas of Amman and Zarqa Figure 6.

Jordan's population became significantly urbanized during the sixties, reaching a rate of urbanization of over 80% in 2011. The two main reasons were rural depopulation and the arrival of waves of Palestinian

refugees and displaced persons who mostly settled in the larger towns of Amman, Zarqa, Irbid and Ruseifa, where UNRWA camps and services had been set up.

Figures 6 to 8 show the country's increasing urbanization between 1979 and 2004. In Jordan the urban threshold is set at a population of 5,000. Note that the localities that are *case* (sub district) centers are considered as towns, regardless of their size. Jordan is characterized by a dense implantation of small towns (with populations of 5,000 to 10,000), which have more than doubled in number over twenty-five years (rising from 26 to 67 towns) (table 4.2-1).

**Table 6: The Distribution of Population According to Locality Size**

Locality size	1979	1994	2004
> 250 000 inhabitants	1	2	3
100 000 - 250 000	2	2	1
50 000 - 100 000	0	5	5
10 000 - 50 000	15	33	45
5 000 - 10 000	26	53	67
1 000 - 5 000	205	268	298
< 1000	898	723	524
	1137	1102	1032

Source: National Population and Housing Census

The number of medium sized towns has tripled (from 15 to 45), mainly in the north and the Jordan Valley. The number of large towns with between 50,000 and 100,000 inhabitants remained stable (five towns) between 1994 and 2004, because in 2004 the Greater Amman Municipality incorporated the eleven fast-growing outlying communities of Abu Nusayr, Shafa Badran, Jubeiha, Sweileh and Tareq in the north, Tala Ali, Badr Jadida and Wadi Sir in the west, Um Qusayr and Kherbet al-Souq in the south and Quweisma in the east.

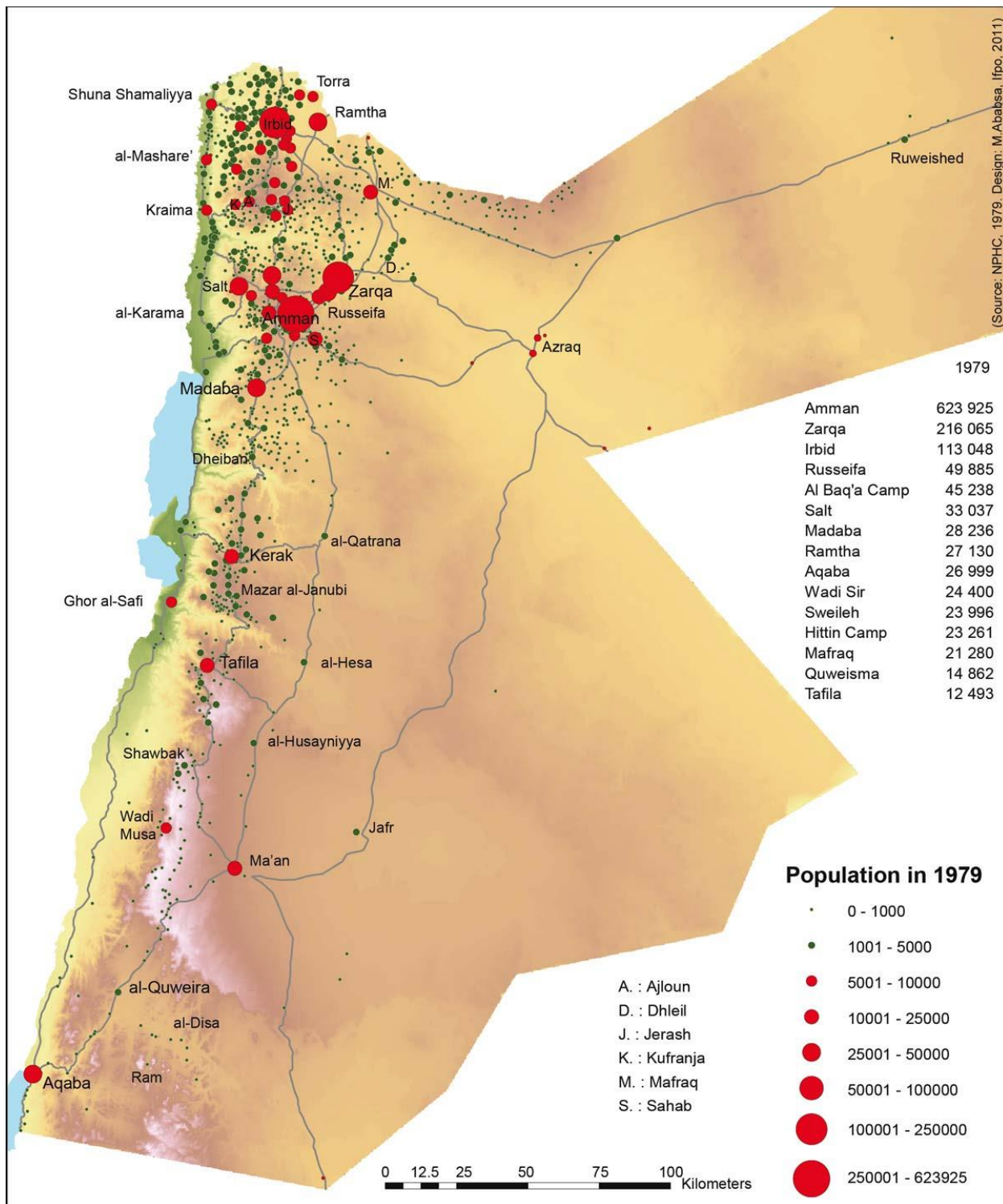
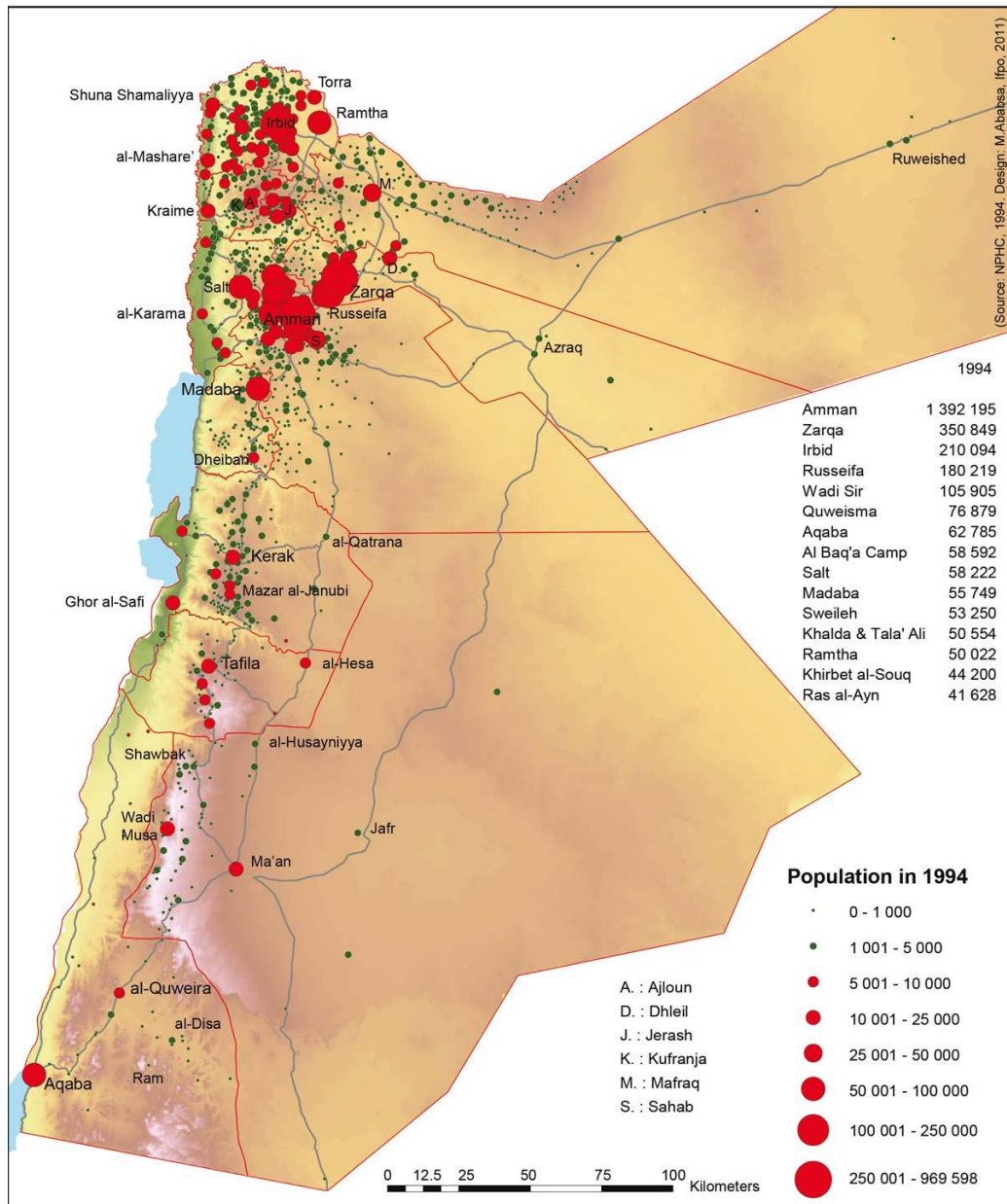


Figure 7: Jordan Population Distribution in Map designed by Myriam Ababsa



**Figure 8: Jordan Population Distribution in 1994**

The urban population of Amman has tripled and that of Ruseifa has risen tenfold since the early 1980s - which coincided with the implementation of structural adjustment policies, with the rise of youth unemployment and the arrival of 300,000 Jordanians of Palestinian origin expelled from the Gulf in 1991. The town of Irbid has expanded and absorbed outlying communities. In contrast, the southern cities of the country have remained stagnant: Kerak’s population rose by only 800 inhabitants between 1994 and 2004 (rising from 18,866 to 19,696), Tafila’s rose by 2,500 (from 20,881 to 23,420) while Ma’an’s fell from 26,731 to 26,124 inhabitants over the same period, reflecting the population drift towards urban areas as well as the crisis in southern Jordan.



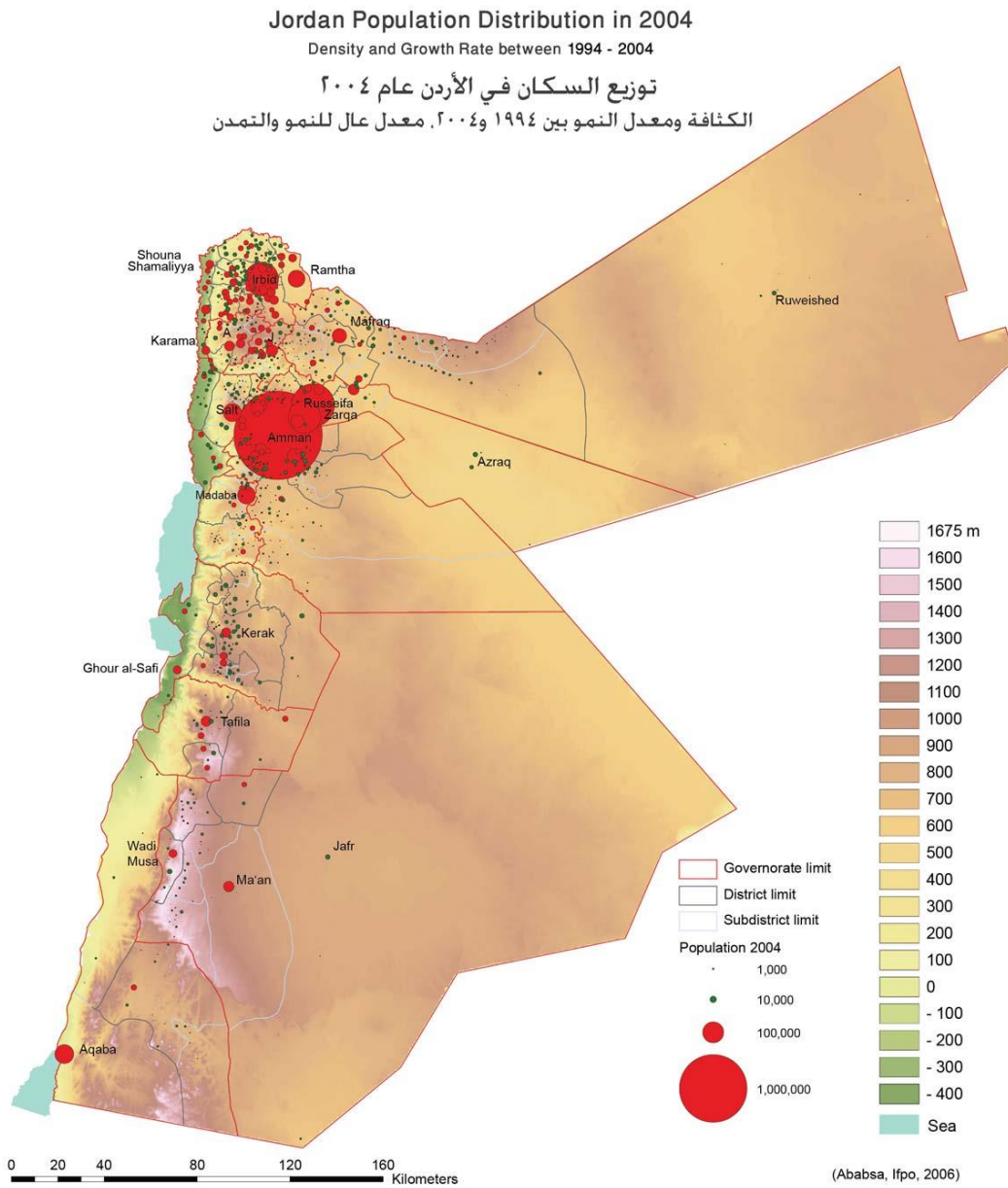


**Figure 10: Jordan Population Distribution in 2004**

**References:**

- Bauer, M.E, Yuan, F. & Saway, K.E., 2003 - Multi-temporal Landsat image classification and change analysis of land cover in the Twin Cities (Minnesota) Metropolitan Area. Second int. workshop on the Analysis of multi-temporal remote sensing images, Italy, pp. 1-8.
- Brown, D. G., Pijanowski, B. C., & Duh, J. D. (2000). Modeling the relationships between land use and land cover on private lands in the Upper Midwest, USA. *Journal of Environmental Management*, 59(4), 247–263. <https://doi.org/10.1006/jema.2000.0369>.
- Burley, T. M. (1961). Land use or land utilization? *Professional Geographer*, 14(5), 18–20.
- Campbell, J. B. (1996). *Introduction to remote sensing* (2nd ed.). London: Taylor and Francis.
- Chica-Olmo, M., & Abarca-Hernandez, F. (2000). Computing geostatistical image texture for remotely sensed data classification. *Computers & Geosciences*, 26(4), 373–383.
- Cohen, Jacob. (1960). A coefficient of agreement for nominal scales. *Educational and Psychological Measurement*, 20(1), 37–46.
- Congalton R.G. Oderwald R.G. Mead R.A. 1983 Assessing Landsat classification accuracy using discrete multivariate analysis statistical techniques.
- David, K., Yetta, G., Agung, F., Sharon, H., & Alison, C. (2016). Land use planning for disaster risk reduction and climate change adaptation: Operationalizing policy and legislation at local levels. *International Journal of Disaster Resilience in the Built Environment*, 7(2), 158–172.
- Diallo, Y., Hu, G., & Wen, X. (2009). Applications of remote sensing in land use/land cover change detection in Puer and Simao Counties, Yunnan Province. *Journal of American Science*, 5(4), 157–166.
- Eren, A., Du'zgu'n, S., & Yalciner, A. C. (2012). Evaluating land use/cover change with temporal satellite data and information systems. *Procedia Technology*, 1, 385–389. <https://doi.org/10.1016/j.protcy.2012.02.079>.
- Foley, J. A., et al. (2005). Global consequences of land use. *Science*, 309(5734), 570. <https://doi.org/10.1126/science.1111772>.
- Foody, G. M. (2002). Status of land cover classification accuracy assessment. *Remote Sensing of Environment*, 80(1), 185–201.
- Herold N., McKerrow A., VanDriel J.N., Wickham J., 2007 -Completion of the 2001 National Land Cover Database for the Conterminous United States. *Photogrammetric Engineering and Remote Sensing*, 73: 337-341.
- Herold, M., Scepan, J., & Clarke, K. C. (2002). The use of remote sensing and landscape-metrics to describe structures and changes in urban land uses. *Environment and Planning A*, 34(8), 1443–1458.
- Homer C., Dewitz J., Fry J., Coan M., Hossain N., Larson C., [http://www.commission4.isprs.org/obia06/Papers/06\\_Automated](http://www.commission4.isprs.org/obia06/Papers/06_Automated)
- Irons, J. R., Dwyer, J. L. & Barsi, J. A. (2012). The next Landsat satellite: The Landsat data continuity mission. *Remote Sensing of Environment*, 122, 11–21.

- Jensen J.R., 2009 - Remote Sensing of the Environment: An Earth Resource Perspective 2/e. Pearson Education India. Jensen, J., 2005 - "Introductory Digital Image Processing, 3<sup>rd</sup> edition".
- Jensen, J. R. (2007). Remote sensing of the environment (2<sup>nd</sup> ed.). Upper Saddle River: Pearson Prentice Hall.
- Ji, W., Ma, J., Twibell, R. W., & Underhill, K. (2005). Characterizing urban sprawl using multi-stage remote sensing images and landscape metrics. *Computers, Environment and Urban Systems*, 30(2006), 861–879.
- Jia, K., Wei, X., Gu, X., Yao, Y., Xie, X., & Li, B. (2014). Landcover classification using Landsat 8 Operational LandImager data in Beijing, China. *Geocarto International*, 29(8), 941–951. <https://doi.org/10.1080/10106049.2014.894586>.
- Kamagata, N., Hara, K., Mori, M., & Akamatsu, Y. (2006) – A new method of vegetation mapping by object-based classification using high resolution satellite.

